JPn Neuroscience
The Journal of Physiology
J Physiol 594.1 (2016) pp 115–134

Hydrogen peroxide modulates synaptic transmission in ventral horn neurons of the rat spinal cord

Masayuki Ohashi[1], Toru Hirano[1], Kei Watanabe[1], Keiichi Katsumi[1], Nobuko Ohashi[2], Hiroshi Baba[2], Naoto Endo[1] and Tatsuro Kohno[2]

[1]*Division of Orthopedic Surgery, Department of Regenerative and Transplant Medicine, Niigata University Graduate School of Medical and Dental Sciences, 1-757 Asahimachi Dori, Chuo-Ku, Niigata City 951-8510, Japan*
[2]*Division of Anesthesiology, Niigata University Graduate School of Medical and Dental Sciences, 1-757 Asahimachi Dori, Chuo-Ku, Niigata City 951-8510, Japan*

Key points

- Excessive production of reactive oxygen species (ROS) is implicated in many central nervous system disorders; however, the physiological role of ROS in spinal ventral horn (VH) neurons remains poorly understood.
- We investigated how pathological levels of H_2O_2, an abundant ROS, regulate synaptic transmission in VH neurons of rats using a whole-cell patch clamp approach.
- H_2O_2 increased the release of glutamate and GABA from presynaptic terminals.
- The increase in glutamate release involved N-type voltage-gated calcium channels (VGCCs), ryanodine receptors (RyRs), and inositol trisphosphate receptors (IP_3Rs); the increase in GABA release, which inhibited glutamatergic transmission, involved IP_3R.
- Inhibiting N-type VGCCs and RyRs attenuates excitotoxicity resulting from increased glutamatergic activity while preserving the neuroprotective effects of GABA, and may represent a novel strategy for treating H_2O_2-induced motor neuron disorders resulting from trauma or ischaemia–reperfusion injury.

Abstract Excessive production of reactive oxygen species (ROS) is a critical component of the cellular and molecular pathophysiology of many central nervous system (CNS) disorders, including trauma, ischaemia–reperfusion injury, and neurodegenerative diseases. Hydrogen peroxide (H_2O_2), an abundant ROS, modulates synaptic transmission and contributes to neuronal damage in the CNS; however, the pathophysiological role of H_2O_2 in spinal cord ventral horn (VH) neurons remains poorly understood, despite reports that these neurons are highly vulnerable to oxidative stress and ischaemia. This was investigated in the present study using a whole-cell patch clamp approach in rats. We found that exogenous application of H_2O_2 increased the release of glutamate from excitatory presynaptic terminals and γ-aminobutyric acid (GABA) from inhibitory presynaptic terminals. The increase of glutamate release was induced in part by an increase in Ca^{2+} influx through N-type voltage-gated calcium channels (VGCCs) as well as by ryanodine receptor (RyR)- and inositol trisphosphate receptor-mediated Ca^{2+} release from the endoplasmic reticulum (ER). In inhibitory presynaptic neurons, increased IP_3R-mediated Ca^{2+} release from the ER increased GABAergic transmission, which served to rescue VH neurons from excessive release of glutamate from presynaptic terminals. These findings indicate that inhibiting N-type VGCCs or RyRs may attenuate excitotoxicity resulting from increased glutamatergic activity while preserving the neuroprotective effects of GABA, and may therefore represent a novel and targeted strategy for preventing and treating H_2O_2-induced motor neuron disorders.

DOI: 10.1113/JP271449

(Resubmitted 15 August 2015; accepted after revision 16 October 2015; first published online 29 October 2015)
Corresponding author T. Kohno: Division of Anesthesiology, Niigata University Graduate School of Medical and Dental Sciences, 1-757 Asahimachi Dori, Chuo-ku, Niigata City 951-8510, Japan. Email: kohno-t@umin.net

Abbreviations ADPR, adenosine diphosphate ribose; 2-APB, 2-aminoethoxydiphenil borate; Bic, bicuculline; BPB, 4-bromophenacyl bromide; CaN, calcineurin; CICR, Ca^{2+}-induced Ca^{2+}-release; CSA, cyclosporine A; Dant, dantrolene sodium; ER, endoplasmic reticulum; IP_3R, inositol trisphosphate receptor; ω-Aga, ω-agatoxin IVA; MPT, mitochondrial permeability transition pore; ω-Ctx, ω-conotoxin GVIA; ROS, reactive oxygen species; RyR, ryanodine receptor; SCI, spinal cord injury; Stry, strychnine; VH, ventral horn; VGCC, voltage-gated calcium channel.

Introduction

Reactive oxygen species (ROS) are generated naturally during cell metabolism, and their levels are tightly regulated by the intracellular antioxidant network in the central nervous system (CNS) and other organs (Giorgio *et al.* 2007; Rice, 2011). However, excessive ROS production is deleterious since it contributes to neuronal damage and degeneration, a hallmark of many pathological conditions of the CNS including trauma, ischaemia–reperfusion injury, and neurodegenerative diseases like amyotrophic lateral sclerosis (ALS) (Halliwell, 1992; Coyle & Puttfarcken, 1993).

Hydrogen peroxide (H_2O_2) is a diffusible and relatively stable ROS that is present in low micromolar concentrations under physiological conditions (Lei *et al.* 1998). H_2O_2 levels are significantly increased in ischaemia–reperfusion lesions of the brain (Hyslop *et al.* 1995) and in spinal cord injury (SCI) (Liu *et al.* 1999). Although the mechanisms of neuronal damage induced by H_2O_2 are not entirely understood, it is known that elevated H_2O_2 levels result in elevated glutamate levels (Mailly *et al.* 1999) and activation of the glutamate receptors including the *N*-methyl-D-aspartate (NMDA) receptor (Mailly *et al.* 1999; Avshalumov & Rice, 2002). The consequent accumulation of high levels of intracellular Ca^{2+} leads to excitotoxicity, which is characterized by neuronal damage and death (Pellegrini-Giampietro *et al.* 1990; Roettger & Lipton, 1996; Shaw & Ince, 1997). Attenuating excitotoxicity is therefore a potential approach for treating CNS injuries and diseases. For instance, riluzole, which reduces overall excitability and neurotransmitter release by inhibiting presynaptic voltage-dependent sodium channels (Leach *et al.* 1986; Doble, 1996), is indicated for use in ALS (Shaw & Ince, 1997) and is being investigated for its therapeutic potential in SCI (Wilson & Fehlings, 2014). However, this class of drugs inhibits not only the release of glutamate but also that of other neurotransmitters including γ-aminobutyric acid (GABA) (Leach *et al.* 1986; Martin *et al.* 1993; Jehle *et al.* 2000). Since GABA provides neuroprotection in cerebral ischaemia via its well-established role in neural inhibition (Schwartz-Bloom & Sah, 2001), selectively inhibiting glutamate release is a better strategy for neuroprotection against excitotoxicity. To date, there has been no study on the effect of H_2O_2 on synaptic transmission in spinal ventral horn (VH) neurons, despite the finding that these neurons are highly vulnerable to oxidative stress (Carri *et al.* 2003) and ischaemia (Sakurai *et al.* 1997; Nohda *et al.* 2007).

The present study investigated the mechanisms by which pathological levels of H_2O_2 affect synaptic transmission in VH neurons using a whole-cell patch clamp approach. We demonstrate that elevated H_2O_2 levels increased glutamate and GABA release from excitatory and inhibitory presynaptic terminals, respectively. The former was partly due to increased presynaptic Ca^{2+} influx through N-type voltage-gated calcium channels (VGCCs) and Ca^{2+} release from the endoplasmic reticulum (ER) mediated by the ryanodine and inositol trisphosphate receptors (RyR and IP_3R, respectively), whereas increased GABAergic transmission was due to IP_3R-mediated Ca^{2+} release from the ER, which inhibited excessive glutamate release from presynaptic terminals.

Methods

Study approval

All experimental procedures involving the use of animals were approved by the Animal Care and Use Committee at Niigata University Graduate School of Medical and Dental Sciences (Niigata, Japan).

Preparation of spinal cord slices

Neonatal Wistar rats of either sex (131 rats, 7–15 days old) were anaesthetized with urethane (1.5 g kg^{-1} by intraperitoneal injection). A dorsal laminectomy was performed and the lumbosacral segment (L1–S3) of the spinal cord was removed (Honda *et al.* 2011). The rats were immediately killed by exsanguination. Spinal cord specimens were placed in pre-oxygenated ice-cold (2–4°C) artificial cerebrospinal fluid (ACSF) containing 117 mM NaCl, 3.6 mM KCl, 2.5 mM $CaCl_2$, 1.2 mM $MgCl_2$, 1.2 mM NaH_2PO_4, 25 mM $NaHCO_3$, and 11.5 mM D-glucose. After cutting the ventral and dorsal roots, the pia-arachnoid membrane was removed, and the spinal cord was mounted on the metal stage of a microslicer (Linear Slicer PRO 7; Dosaka, Kyoto, Japan) and cut into 500 μm transverse

slices. Each of these was transferred to a recording chamber and placed on the stage of an upright microscope equipped with an infrared–differential interference contrast (IR-DIC) system (E600FN; Nikon, Tokyo, Japan). The slice was fixed with an anchor and superfused at 5–6 ml min^{-1} with ACSF equilibrated with a gas mixture of 95% O_2 and 5% CO_2 (pH 7.4), with the temperature maintained at 36 ± 0.5°C using a temperature controller (TC-324B; Warner Instruments, Hamden, CT, USA). Slices were used for recording after a recovery period of ≥ 40 min.

Patch clamp recordings from spinal VH neurons

Laminar regions were identified under low magnification (5× objective) and individual neurons were identified using the 40× objective lens of an IR-DIC microscope and monitored with a charge-coupled device camera (C2400-79H; Hamamatsu Photonics, Hamamatsu, Japan). Whole-cell patch clamp recordings were made from the large VH neurons of Rexed lamina IX (size: > 25 μm), which were most frequently seen in the ventrolateral and ventromedial areas. A somal size > 20 μm was used as the cut-off in past studies of postnatal rat lumbar motor neurons (Takahashi, 1990); however, large interneurons (> 20 μm) have been detected in the ventral half of the rat lumbar spinal cord (Thurbon *et al.* 1998*a*,*b*). Therefore, putative motor neurons were identified as the largest cells in the VH (somal diameter > 25 μm). After the whole-cell configuration was established, neurons were held in voltage-clamp at −70 mV to record excitatory postsynaptic currents (EPSCs) or at 0 mV for recording inhibitory postsynaptic currents (IPSCs). In spinal VH neurons, the reversal potentials of EPSCs are 0 mV, and those of IPSCs are −70 mV (Aoyama *et al.* 2010; Honda *et al.* 2012; Yamamoto *et al.* 2012). Therefore, EPSCs in the membrane current trace were specifically recorded as downward deflections at −70 mV, while IPSCs were specifically recorded as upward deflections at 0 mV. Cell input resistance (R_{in}) was calculated by measuring the current response to 5 mV hyperpolarizing steps from a −70 mV holding potential (Pagnotta *et al.* 2005; Quitadamo *et al.* 2005). To investigate the effects of H_2O_2 on presynaptic terminals of fibres synaptically connected to the VH neuron being recorded, all patch clamp recordings were made in the presence of the Na^+ channel blocker tetrodotoxin (TTX; 1μM). Since conduction of action potentials is blocked by TTX, the effects of H_2O_2 on presynaptic terminals could be isolated. In the presence of TTX, postsynaptic responses to spontaneously released neurotransmitters were detected as miniature (m) EPSCs and mIPSCs. Whole-cell patch clamp pipettes were constructed from borosilicate glass capillaries (1.5 mm outer diameter; World Precision Instruments, Sarasota, FL, USA). The resistance of a typical pipette was 4–8 MΩ when filled with internal solution composed of 110 mM Cs_2SO_4, 5 mM tetraethylammonium, 0.5 mM $CaCl_2$, 2 mM $MgCl_2$, 5 mM EGTA, 5 mM Hepes and 5 mM ATP-Mg.

Signals were amplified with an Axopatch 200B amplifier (Molecular Devices, Union City, CA, USA), filtered at 2 kHz, and digitized at 5 kHz. Data were stored and analysed using the pCLAMP 10.3 data acquisition program (Molecular Devices).

Drug application

The following pharmacological agents were purchased from Wako (Osaka, Japan): H_2O_2 (1 mM), TTX (1 μM), CGP35348 (20 μM), dantrolene sodium (Dant; 10 μM), 2-aminoethoxydiphenyl borate (2-APB; 200 μM), flufenamic acid (FFA; 100 μM), 4-bromophenacyl bromide (BPB; 20 μM), cyclosporine A (CSA; 10 μM), nifedipine (10 μM), ω-conotoxin GVIA (ω-Ctx; 0.5 μM), and SNX-482 (0.1 μM). Bicuculline (Bic; 20 μM), strychnine (Stry; 2 μM), and ω-agatoxin IVA (ω-Aga; 0.2 μM) were purchased from Sigma-Aldrich (St Louis, MO, USA). H_2O_2 was freshly dissolved in ACSF immediately before the experiments. TTX, Stry, CGP35348, ω-Aga and ω-Ctx were first dissolved in distilled water at 1000 times the working concentration. Bic, Dant, 2-APB, BPB, CSA, nifedipine and SNX-482 were dissolved in dimethyl sulfoxide at a 1000 times the concentration for storage, and then diluted to the working concentration in ACSF immediately before use. The osmotic pressure of nominally Ca^{2+}-free, high-Mg^{2+} (5 mM) ACSF was adjusted by lowering the Na^+ concentration. Drugs were applied to the whole slice by perfusion via a three-way stopcock without changing the perfusion rate or temperature. The volume of the recording chamber was approximately 1.0 ml. The drugs reached the recording chamber within 15 s of opening the stopcock and were completely washed out within 90 s of its being closed. Both the test inhibitor and TTX were superfused at least 4 min before starting H_2O_2 superfusion. Since the focus of the present study was on the acute toxicity of ROS, H_2O_2 was applied for 5 min at a concentration of 1 mM, which was previously shown to induce neurotoxicity in spinal neurons (Taccola *et al.* 2008) and hypoglossal motoneurons (Nani *et al.* 2010) *in vitro*. Slices were discarded after each H_2O_2 application experiment.

Data analysis

Changes in frequency of postsynaptic currents following bath application of drugs were analysed by determining the time course of postsynaptic current frequency and amplitude before and after drug application with a time bin of 30 s using the Mini Analysis program 6.0.7 (Synaptosoft, Decatur, GA, USA). The threshold for detection of postsynaptic currents was set at 2 times the

root mean square of the background noise and each automatically identified event was visually confirmed to be free of artefacts.

Statistics

All numerical data are expressed as the mean ± SEM. Student's *t* test (paired or unpaired) or one-way analysis of variance (ANOVA) with a Bonferroni *post hoc* test was used to determine the statistical significance between means. The Kolmogorov–Smirnov test was used to compare cumulative distributions of postsynaptic current parameters in the absence and presence of the drugs. $P < 0.05$ was considered significant for all tests. For electrophysiological data, the number of samples n refers to the number of neurons recorded.

Results

H_2O_2 acts presynaptically to modulate spontaneous glutamate release in VH neurons

To determine whether H_2O_2 directly modulates excitatory neuronal activity, we measured mEPSCs under whole-cell patch clamp at a holding potential of −70 mV in the presence of TTX. The mEPSCs had an average frequency of 9.5 ± 1.0 Hz and an average amplitude of 11.3 ± 0.5 pA ($n = 11$). H_2O_2 superfusion for 5 min produced biphasic changes in the frequency from baseline, specifically, an increase (maximum: 163.1 ± 10.9 % of the control) followed by a depression (51.7 ± 6.5% of the control) that persisted for at least 10 min following washout (Fig. 1*A*–*C*). The maximal increase in frequency was observed 2–5.5 min after the start of H_2O_2 superfusion (mean = 3.6 ± 0.3 min) (Fig. 1*B*). In contrast, mEPSC amplitude was unaffected by H_2O_2 treatment (Fig. 1*C*, right panel). Figure 1*D* shows that H_2O_2 increased the proportion of mEPSCs with a shorter inter-event interval relative to the control (Kolmogorov–Smirnov test), and those with longer inter-event intervals were observed for at least 10 min after the washout (left panel). However, H_2O_2 had no effect on the cumulative distribution of mEPSC amplitude over the recording period (Fig. 1*D*, right panel).

We next examined the effect of H_2O_2 treatment on R_{in}. Bath-application of H_2O_2 (1 mM; 5 min) did not affect R_{in} values, which were 144.4 ± 40.9 MΩ before H_2O_2 superfusion, 138.9 ± 38.0 MΩ after 5 min of H_2O_2 superfusion (98.3 ± 2.1% of the control, paired *t* test, $P = 0.47$, $n = 6$), and 147.5 ± 42.3 MΩ after 10 min of H_2O_2 washout (101.5 ± 1.8% of the control, paired *t* test, $P = 0.44$, $n = 6$), when measured from the same neurons before and after application. Moreover, to examine whether the depression phase of mEPSC frequency simply reflected damage to release machinery, we investigated the influence of a prolonged (15 min) application of H_2O_2 (Fig. 2*A*). At 15 min after H_2O_2 superfusion, the increase of mEPSC frequency was sustained relative to control values, which are written in square brackets at their first mention (165.3 ± 21.4% of the control [12.8 ± 3.3 Hz], paired *t* test, $P = 0.016$, $n = 7$). This was followed by a depression that persisted for at least 10 min following washout (42.1 ± 8.4% of the control, paired *t* test, $P = 0.001$, $n = 6$; Fig. 2*B*, left panel). In contrast, mEPSC amplitude was not affected significantly when compared with the control (Fig. 2*B*, right panel).

H_2O_2 increases mEPSC frequency by causing an elevation in presynaptic Ca^{2+} concentration

We next investigated the mechanism underlying the H_2O_2-induced increase in mEPSC frequency. Given that the frequency of spontaneous miniature synaptic events correlates with presynaptic Ca^{2+} concentration (Augustine *et al.* 2003), we investigated the source of presynaptic Ca^{2+}. In general, these include influx through VGCCs in the plasma membrane (Catterall & Few, 2008) and release from the ER, which stores intracellular Ca^{2+}. ER release is mediated by RyR or IP_3R (Verkhratsky, 2002), whereas the mitochondria also play a role in regulating presynaptic Ca^{2+} concentration (Zenisek & Matthews, 2000; Billups & Forsythe, 2002).

Owing to the presence of exposed sulfhydryl groups, several ion channels and receptors including VGCCs (Nowicky AV & Duchen MR, 1998), RyR and IP_3R (Gerich *et al.* 2009) are activated by changes in cytosolic redox balance and by the level of ROS such as H_2O_2. We therefore investigated the role of VGCC-, mitochondria-, RyR-, and IP_3R-mediated Ca^{2+} signalling on H_2O_2-induced excitatory activity by patch clamp combined with pharmacological manipulations. As a control, we recorded from cells exposed to both the inhibitor of interest and TTX but not H_2O_2. The values of the control are written in square brackets at their first mention. Given that the maximal increases in mEPSC frequency induced by H_2O_2 were observed between 2 and 5.5 min after the start of H_2O_2 superfusion, we evaluated maximal mEPSC frequency 1.5–6 min after superfusion.

We first examined whether H_2O_2-induced increases in mEPSC frequency were dependent on extracellular Ca^{2+}. In Ca^{2+}-free ACSF, H_2O_2 superfusion had little effect on mEPSC frequency (102.8 ± 6.1% of the control [8.4 ± 2.1 Hz]; paired *t* test, $P = 0.66$, $n = 7$; Fig. 3*A* and *B*), suggesting that influx through VGCCs was partly responsible for the increase in intracellular Ca^{2+} level. In contrast, the subsequent depression in mEPSC frequency (48.9 ± 7.8% of the control; paired *t* test, $P = 0.0006$,

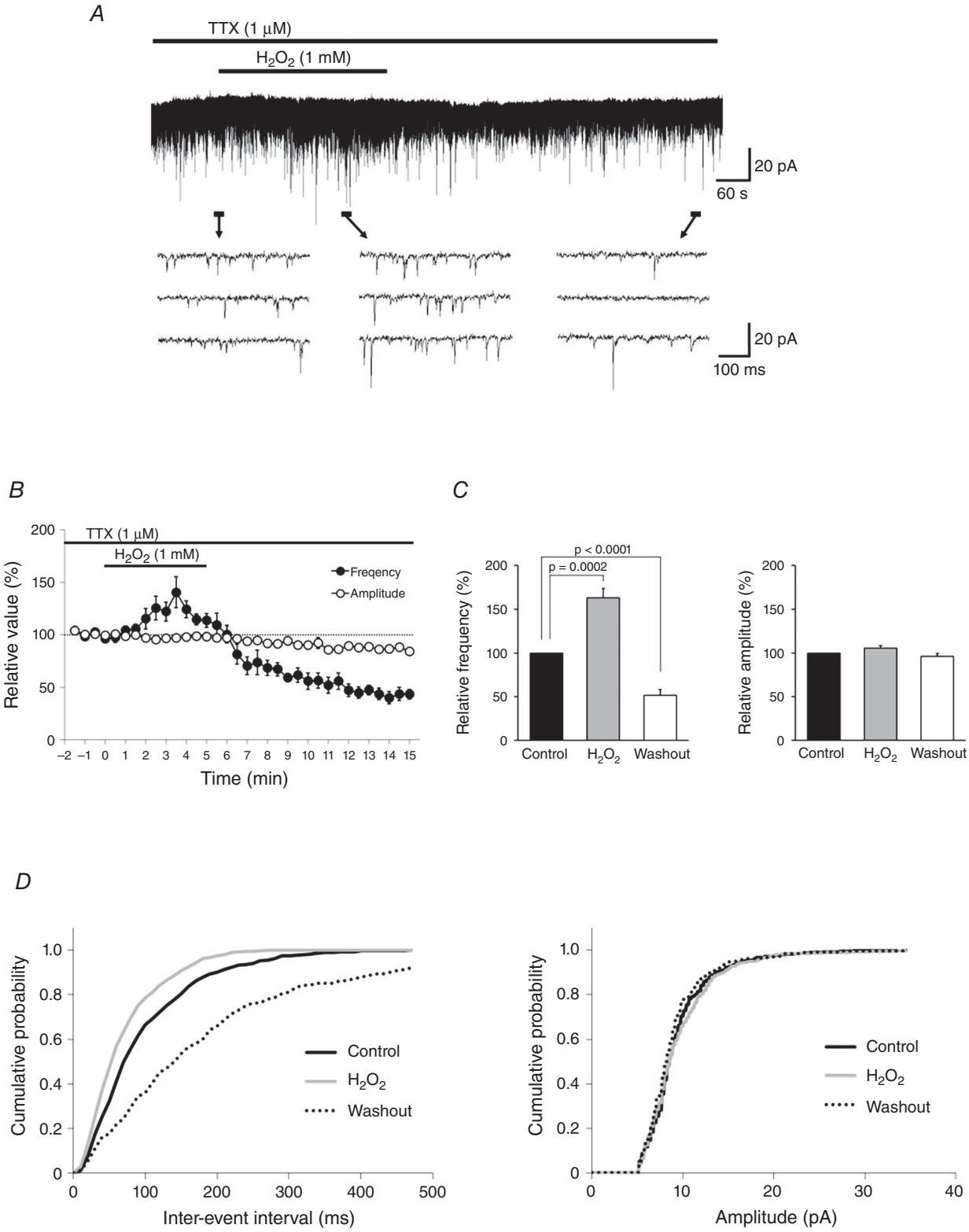

Figure 1. H_2O_2 induces an increase followed by depression in mEPSC frequency without affecting amplitude

A, continuous chart recording of mEPSCs before, during and after H_2O_2 (1 mM) superfusion. *B*, average frequency (filled circles) and amplitude (open circles) of mEPSCs in the presence of H_2O_2 relative to the control, shown as a function of time (mean ± SEM, $n = 11$). *C*, summary of mEPSC frequency (left) and amplitude (right). Values are

$n = 7$) was not prevented in Ca^{2+}-free ASCF (i.e. was the same as observed in standard ACSF) (Fig. 3*A* and *B*).

Multiple types of VGCCs are expressed throughout the CNS (Frank, 2014); an immunocytochemical analysis revealed that rat spinal VH neurons express L-, P/Q-, N- and R-type VGCCs (Westenbroek *et al.* 1998), although the presynaptic input to these cells presumably involves a different constellation of VGCCs. To determine the contribution of different presynaptic VGCC subtypes on the H_2O_2-induced increase in spontaneous mEPSCs at excitatory synapses, we used VGCC inhibitors specific for each channel type during H_2O_2 superfusion of VH neurons.

Nifedipine, a dihydropyridine antagonist of L-type VGCCs, had no effect on the H_2O_2-induced increase in mEPSC frequency (173.3 ± 18.8% of the control [10.8 ± 1.8 Hz], $n = 7$). In contrast, inhibiting P/Q- or R-type VGCCs with ω-Aga and SNX-482, respectively, partially blocked this increase (ω-Aga, 125.5 ± 10.6% of the control [10.1 ± 1.0 Hz], $n = 6$, Fig. 3*C*; SNX-482, 132.6 ± 6.2% of the control [8.2 ± 1.2 Hz], $n = 6$), while a complete suppression was observed by blocking N-type VGGCs with ω-Ctx (97.7 ± 5.6% of the control [12.3 ± 2.5 Hz], $n = 6$; Fig. 3*D*). A comparison between values obtained using VGCC inhibitors and TTX only by one-way ANOVA revealed a significant effect of ω-Ctx ($F_{5,38} = 7.73$, $P < 0.0001$; Bonferroni *post hoc* test, TTX only *vs.* ω-Ctx, $P = 0.0001$; Fig. 3*E*). These VGCC blockers did not block the subsequent depression of mEPSC frequency observed after H_2O_2 washout (Nifedipine, 52.0 ± 10.6% of the control, $n = 6$; ω-Aga, 52.8 ± 10.8% of the control, $n = 5$; ω-Ctx, 58.5 ± 10.0% of the control, $n = 6$; SNX-482, 61.3 ± 7.0% of the control, $n = 6$).

To determine whether intracellular Ca^{2+} stores are activated by H_2O_2, we targeted mitochondria and the ER using specific inhibitors. CSA, which blocks the opening of the mitochondrial permeability transition pore (MPT), had no effect on H_2O_2-induced changes in mEPSC frequency (with H_2O_2 superfusion, 168.3 ± 15.3% of the control [7.4 ± 1.3 Hz]; after washout, 54.2 ± 6.2% of the control; $n = 6$ each). CSA also inhibits calcineurin (CaN). Therefore, these results further suggest that CaN does not mediate H_2O_2-induced changes in mEPSC frequency in spinal VH neurons.

We then tested whether H_2O_2 affects intracellular Ca^{2+} release from the ER, which is mediated by RyR and IP_3R. Dant, an RyR inhibitor, blocked the increase in mEPSC frequency induced by H_2O_2 (92.9 ± 8.3% of the control [8.1 ± 1.4 Hz], $n = 8$), but did not alter the subsequent decrease in frequency after H_2O_2 washout (42.7 ± 7.6% of the control, $n = 5$; Fig. 4*A*). In the presence of 2-APB, an IP_3R antagonist, the H_2O_2-induced increase in mEPSC frequency not only was blocked but was reduced after 5 min, reaching a maximum value between 1.5 and 6 min after the start of superfusion to 81.2 ± 11.0% of the control [12.7 ± 2.0 Hz] ($n = 6$; Fig. 4*B*). These changes were accompanied by an outward current (> 5 pA) in five of six neurons (14.2 ± 1.6 pA, $n = 5$; Fig. 4*B*). The decrease in mEPSC frequency was reversible, and subsequent depression of mEPSC frequency by H_2O_2 was completely blocked (99.5 ± 7.0% of the control, $n = 6$; Fig. 4*B*). H_2O_2 treatment in the presence of 2-APB had no effect in recordings of another five neurons: the R_{in} values were 146.9 ± 31.9 MΩ before H_2O_2 superfusion, 150.24 ± 32.5 MΩ after 5 min of H_2O_2 superfusion (102.3 ± 2.5% of the control, paired *t* test, $P = 0.42$, $n = 5$), and 142.9 ± 29.2 MΩ after 10 min of H_2O_2 washout (98.5 ± 3.6% of the control, paired *t* test, $P = 0.69$, $n = 5$).

A comparison between values obtained with CSA, Dant, or 2-APB and TTX only by one-way ANOVA showed significant effects of Dant and 2-APB on the H_2O_2-induced increase in mEPSC frequency ($F_{4,31} = 12.5$, $P < 0.0001$; Bonferroni *post hoc* test, TTX only *vs.* Dant or 2-APB, $P < 0.0001$ for each; Fig. 4*C*, left panel), and a significant effect of 2-APB on the subsequent depression ($F_{3,23} = 11.8$, $P < 0.0001$; Bonferroni *post hoc* test, TTX only *vs.* 2-APB, $P < 0.0001$; Fig. 4*C*, right panel).

Although we used 2-APB as an IP_3 antagonist in this experiment, 2-APB also blocks Na^+ and Ca^{2+}-permeable melastatin-related transient receptor potential 2 (TRPM2) channels (Xu *et al.* 2005; Togashi *et al.* 2008). We therefore examined the effect of another TRPM2 channel blocker, flufenamic acid (FFA) (Hill *et al.* 2004; Naziroğlu *et al.* 2011; Lee *et al.* 2011, 2013), on the H_2O_2-induced changes of mEPSC frequency (Fig. 4*D*). FFA (100 μM) did not block the initial H_2O_2-induced increased of mEPSC frequency (171.5 ± 10.1% of control [13.4 ± 2.5 Hz], paired *t* test, $P = 0.0004$, $n = 7$) or the subsequent depression after

shown as percentage change in maximal values relative to the control during H_2O_2 superfusion and after washout (mean ± SEM, $n = 11$ each). *P* values were determined by a paired *t* test. *D*, cumulative distributions of the mEPSC inter-event interval (left) and amplitude (right) before (continuous black line), during (grey line), and after (dotted line) H_2O_2 superfusion. Values were compared to the control with the Kolmogorov–Smirnov test. H_2O_2 had no effect on amplitude (during H_2O_2 superfusion: $P = 0.13$; after washout: $P = 0.78$), but inter-event interval was shorter during H_2O_2 superfusion ($P < 0.0001$) and longer after washout ($P < 0.0001$). *A* and *D* were obtained from the same neuron. The holding potential was −70 mV for all recordings. Washout indicates the 10 min period after initiating H_2O_2 washout.

H_2O_2 washout (61.5 ± 11.0% of the control, paired *t* test, $P = 0.025$, $n = 7$) (Fig. 4*E*).

IP_3, the natural ligand for IP_3R, arises from the enzymatic activity of phospholipase C (PLC)-β, which is downstream of G protein-coupled receptor activation, as detailed in Fig. 8 (Rhee & Bae, 1997). We therefore examined the effect of the PLC/A_2 inhibitor BPB on the H_2O_2-induced increase and subsequent depression in mEPSC frequency. Unlike the IP_3R antagonist 2-APB, BPB did not block this increase (167.8 ± 15.4% of the control [13.6 ± 3.5 Hz], paired *t* test, $P = 0.0071$, $n = 6$) and subsequent depression (59.5 ± 6.5% of the control, paired *t* test, $P = 0.0034$, $n = 5$), indicating that H_2O_2-mediated IP_3R-related signalling is downstream of PLC-β.

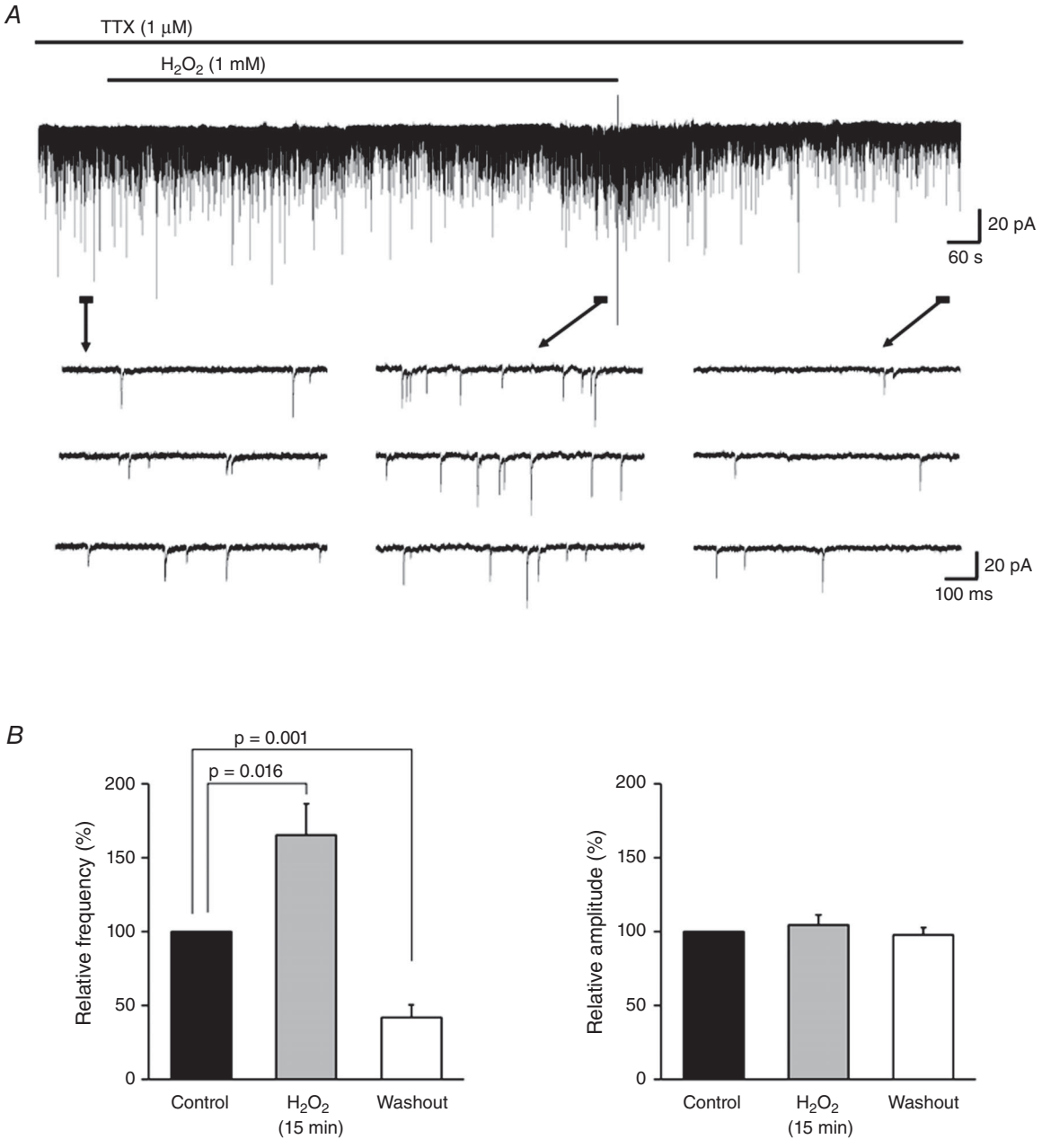

Figure 2. Prolonged application of H_2O_2 results in an increase followed by depression in mEPSC frequency
A, continuous chart recording of mEPSCs before, during and after H_2O_2 (1 mM, 15 min) superfusion. *B*, summary of mEPSC frequency data. Values are shown as percentage change relative to the control after 15 min of H_2O_2 superfusion ($n = 7$) and after washout ($n = 6$) (mean ± SEM). *P* values were determined by a paired *t* test. The holding potential was −70 mV for all recordings. Washout indicates the 10 min period after initiating H_2O_2 washout.

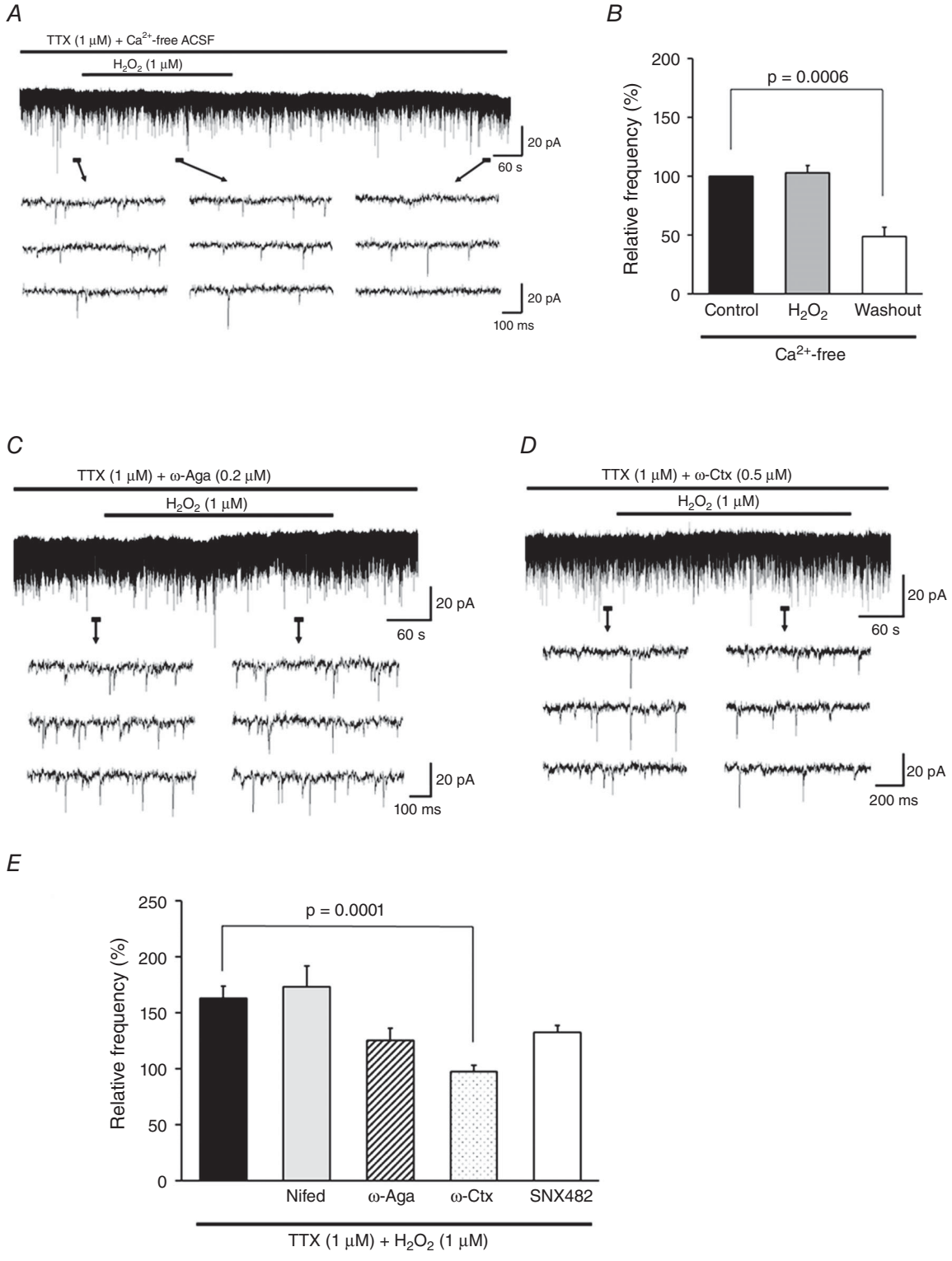

Figure 3. H_2O_2 induces an increase in mEPSC frequency by modulating Ca^{2+} influx via N-type VGCCs
A, effect of H_2O_2 on mEPSCs in Ca^{2+}-free ACSF. Under this condition, the H_2O_2-induced mEPSC increase but not its subsequent depression was completely blocked. *B*, summary of mEPSC frequency in Ca^{2+}-free ACSF (mean ± SEM, $n = 7$). Values in the charts correspond to percentage change in maximal values of mEPSC

H_2O_2-induced enhancement of GABAergic activity reduces mEPSC frequency following the initial increase

In spinal dorsal horn neurons, ischaemia leads to an increase in the release of GABA and glycine (Kawasaki *et al.* 2004) and a decrease in glutamate release from nerve terminals via activation of GABA receptors (Matsumoto *et al.* 2003). H_2O_2-induced increases in GABA release have also been reported in the spinal dorsal horn (Takahashi *et al.* 2007). Based on these findings, we investigated whether GABA and/or glycine receptors at presynaptic terminals are involved in the depression of mEPSC frequency by H_2O_2 using specific receptor antagonists.

GABA receptors are ionotropic A-type ($GABA_A$) or metabotropic G protein-coupled B-type ($GABA_B$) (Kumamoto, 1997), and both receptors have been detected in nerve terminals of spinal motor neurons (Rekling *et al.* 2000). The addition of Bic or CGP35348 – $GABA_A$ and $GABA_B$ receptor antagonists, respectively – led to a robust enhancement of the H_2O_2-mediated increase in mEPSC frequency (Bic, 241.1 ± 37.3% of the control [7.3 ± 1.8 Hz], $n = 7$; CGP35348, 282.3 ± 69.4% of the control [7.1 ± 0.7 Hz], $n = 6$; Fig. 5*A* and *B*). The subsequent depression in mEPSC frequency was blocked by Bic (108.7 ± 10.7% of the control, $n = 7$; Fig. 5*A*) but not by CGP35348 (48.2 ± 12.2% of the control, $n = 6$; Fig. 5*B*). Treating neurons with the glycine receptor antagonist Stry had no effect on H_2O_2-mediated changes in mEPSC (during H_2O_2 superfusion, 162.6 ± 19.5% of the control [8.6 ± 1.1 Hz]; after washout, 44.9 ± 7.3% of the control; $n = 6$ for each; Fig. 5*C*). A comparison between values obtained with Bic, CGP35348, or Stry and TTX only revealed a trend of enhanced H_2O_2-induced increases in mEPSC frequency in the presence of Bic or CGP35348; however, the differences were not statistically significant (one-way ANOVA, $F_{3,26} = 2.86$, $P = 0.056$; Fig. 5*D*, left panel). In contrast, Bic had a significant effect on the subsequent depression of mEPSC frequency (one-way ANOVA, $F_{3,26} = 11.05$, $P < 0.0001$; Bonferroni *post hoc* test, TTX only *vs.* Bic, $P < 0.0001$; Fig. 5*D*, right panel). These data suggest that $GABA_A$ and $GABA_B$ receptor activation in terminals that innervate VH neurons inhibits the excessive presynaptic release of glutamate induced by H_2O_2 superfusion, and that $GABA_A$ receptor activation is involved in the subsequent depression in mEPSC frequency.

H_2O_2 increases the frequency of GABAergic miniature inhibitory postsynaptic currents (mIPSCs)

The above findings prompted us to examine the effects of H_2O_2 on GABA release from presynaptic terminals by recording GABAergic mIPSCs in VH neurons. Since GABA and glycine are both released from axon terminals that synapse on spinal motor neurons (Ornung *et al.* 1994; Taal & Holstege, 1994; Jonas *et al.* 1998; Baer *et al.* 2003), GABAergic mIPSCs were isolated by adding TTX and Stry to the ACSF.

GABAergic mIPSCs were measured at a holding potential of 0 mV; the frequency and amplitude were 1.9 ± 0.4 Hz and 10.0 ± 0.7 pA, respectively ($n = 8$). H_2O_2 superfusion resulted in a marked increase in frequency (647.8 ± 201.4% of the control) but only a minimal change in amplitude (120.0 ± 8.3% of the control; paired *t* test, $P = 0.057$; Fig. 6*A* and *C*). These changes were accompanied by a more than 5 pA of outward current in seven of eight neurons examined (25.0 ± 10.1 pA, $n = 7$; Fig. 6*A*). Figure 6*B* shows the time course of the average change in GABAergic mIPSC frequency and amplitude in response to H_2O_2. The maximal increase in frequency was delayed, appearing 4.5–7 min (mean = 5.9 ± 0.4 min) after initiating H_2O_2 superfusion or approximately 2 min after initiating the washout (Fig. 6*C*). The effect was reversible, but persisted for 10 min after the washout (Fig. 6*C*); it also coincided with the decrease in mEPSC frequency observed after H_2O_2 washout (Fig. 1*B*). These results suggest that changes in mEPSCs induced by H_2O_2 are mediated by GABA. Figure 6*D* shows that H_2O_2 application shortened the average inter-event interval without causing a significant change in amplitude relative to the control (during H_2O_2 superfusion: frequency, $P < 0.0001$; amplitude, $P = 0.051$; after washout: frequency, $P < 0.0001$; amplitude, $P = 0.061$; Kolmogorov–Smirnov test).

H_2O_2-induced increase in GABAergic mIPSC frequency involves intracellular Ca^{2+} release via IP_3R

We next examined the role of Ca^{2+} signalling in the modulation of GABAergic mIPSC frequency by H_2O_2.

frequency relative to the control during H_2O_2 superfusion and after washout. The *P* value was determined by a paired *t* test. *C*, ω-Aga (0.2 μM), a P/Q-type VGCC blocker, partially suppressed the H_2O_2-induced increase in mEPSC frequency. *D*, ω-Ctx (0.5 μM), an N-type VGCC blocker, completely suppressed the increase in frequency. *E*, summary of mEPSC frequencies observed during H_2O_2 superfusion with TTX alone ($n = 11$) or with nifedipine (L-type VGCC blocker, 10 μM; $n = 7$), ω-Aga (0.2 μM; $n = 6$), ω-Ctx (0.5 μM; $n = 6$), or SNX-482 (R-type VGCC blocker, 0.1 μM; $n = 6$) relative to control (mean ± SEM). Maximal values of mEPSC frequency relative to the control 1.5–6 min after H_2O_2 superfusion are shown. *P* values were determined by one-way ANOVA with a Bonferroni *post hoc* test. The holding potential was −70 mV for all recordings. Washout indicates the 10 min period after initiating H_2O_2 washout.

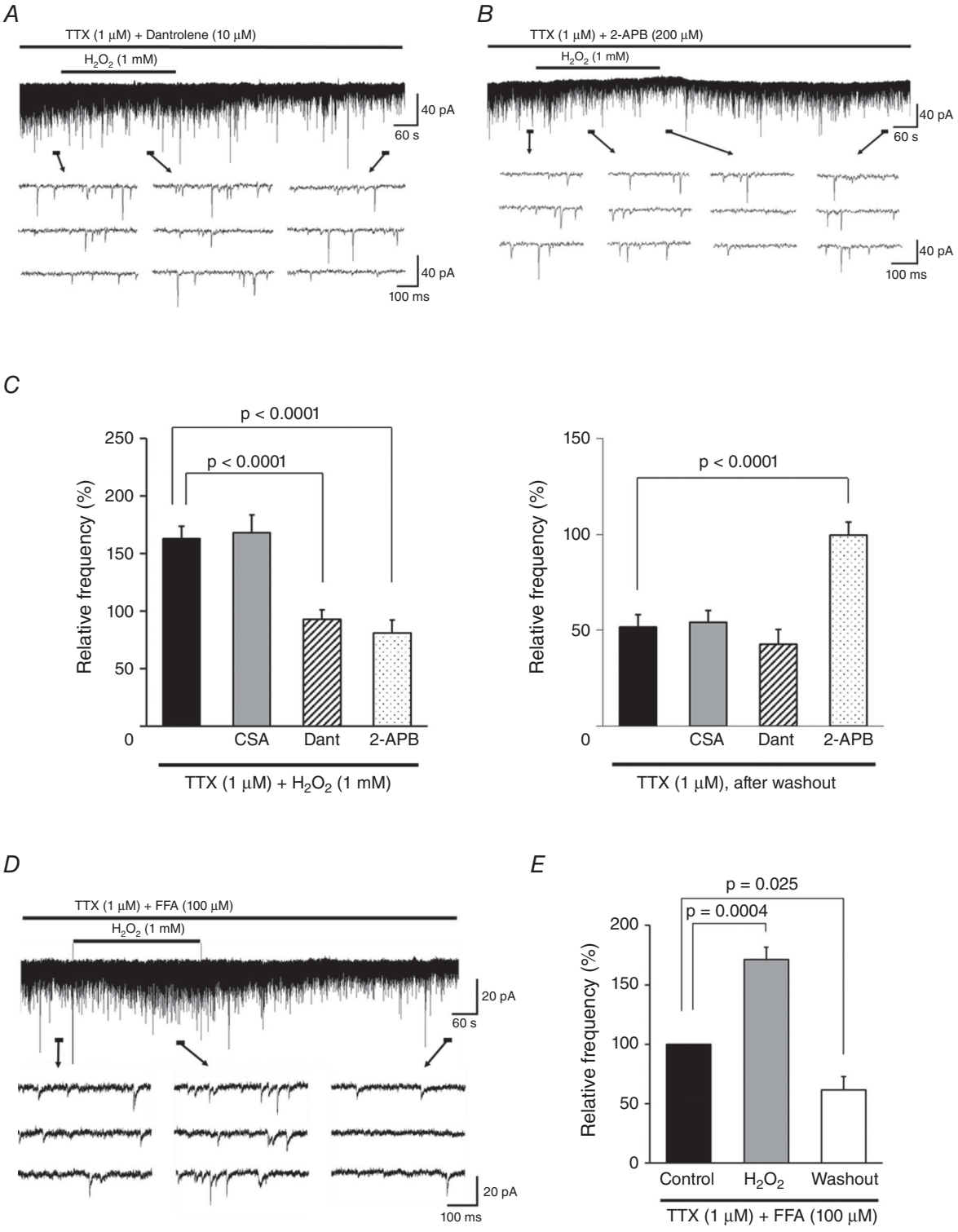

Figure 4. H_2O_2-induced increases in mEPSC frequency are due to intracellular Ca^{2+} release via RyR and IP3R

A, Dant (10 μM), an RyR antagonist, completely blocked the H_2O_2-induced increase in mEPSC frequency but not the subsequent depression. *B*, the IP_3R antagonist 2-APB (200 μM) completely blocked both the increase and depression in frequency. Note that the increase not only was blocked but was reduced with respect to the control

In Ca^{2+}-free ACSF, H_2O_2 superfusion increased the frequency of GABAergic mIPSCs (413.0 ± 94.2% of the control [1.6 ± 0.2 Hz], $n = 6$; Fig. 7*A* and *B*) to a level similar to that observed in normal ACSF ($P = 0.36$, unpaired *t* test), indicating that Ca^{2+} influx is not involved in the H_2O_2-induced increase in GABA release. The effect was reversible, but persisted for 10 min after the washout (181.2 ± 29.4% of the control, $n = 6$). In addition, the H_2O_2-induced increase of GABAergic mIPSC frequency was accompanied by an outward current (> 5pA) in three of six neurons examined (18.1 ± 10.9 pA, $n = 3$).

We then pharmacologically targeted mitochondria and the ER to determine whether intracellular Ca^{2+} stores are activated by H_2O_2 at GABAergic inhibitory presynaptic terminals. CSA (an MPT blocker/calcineurin inhibitor) and Dant (an RyR antagonist) had no effect on H_2O_2-induced increases in mIPSC frequency during H_2O_2 superfusion (CSA, 373.6 ± 72.5% of the control [1.8 ± 0.4 Hz], $n = 6$; Dant, 352.0 ± 63.3% of the control [2.1 ± 0.7 Hz], $n = 6$) and after H_2O_2 washout (CSA, 202.3 ± 34.1% of the control, $n = 6$; Dant, 184.6 ± 30.2% of the control, $n = 6$). Moreover, H_2O_2-induced outward currents (> 5 pA) were seen in three of six neurons treated with CSA (17.4 ± 9.5 pA, $n = 3$) and in four of six neurons treated with Dant (28.5 ± 12.7 pA, $n = 4$). In contrast, 2-APB (an IP_3R antagonist) completely blocked H_2O_2-induced increases in mIPSC frequency during H_2O_2 superfusion (106.6 ± 11.8% of the control [2.1 ± 0.4 Hz], $n = 7$) and after H_2O_2 washout (101.0 ± 12.8% of the control, $n = 5$) as well as the outward current (Fig. 7*C*). A comparison between values during H_2O_2 superfusion obtained for CSA, Dant, or 2-APB and TTX + Stry only showed a significant effect of 2-APB ($F_{3,23} = 3.31$, $P = 0.038$; one-way ANOVA with Bonferroni *post hoc* test, *vs.* TTX + Stry, $P = 0.0046$; Fig. 7*D*). Moreover, the H_2O_2-induced increase of GABAergic mIPSC frequency was not blocked by the application of the TRPM2 channel blocker FFA (during H_2O_2 superfusion, 528.1 ± 92.8% of the control [2.2 ± 0.7 Hz], paired *t* test, $P = 0.0058$, $n = 6$, Fig. 7*E* and *F*; after H_2O_2 washout, 188.4 ± 20.5% of the control, paired *t* test, $P = 0.0076$, $n = 6$; accompanied by an outward current (> 5 pA) in four of six neurons (22.0 ± 6.5 pA, $n = 4$; Fig. 7*E*)). These results suggest that the IP_3R-sensitive pool in the ER is the source of the Ca^{2+} responsible for the increase in GABAergic mIPSC frequency. However, this was not blocked by the application of the PLC-β inhibitor BPB (during H_2O_2 superfusion, 503.7 ± 95.6% of the control [1.9 ± 1.1 Hz], paired *t* test, $P = 0.0083$, $n = 6$; after H_2O_2 washout, 224.7 ± 40.4% of the control, paired *t* test, $P = 0.027$, $n = 6$), indicating that H_2O_2 acts downstream of PLC-β, as in the case of mEPSCs.

Discussion

The present study investigated the cellular mechanisms underlying the effects of H_2O_2 on synaptic transmission in spinal VH neurons. We demonstrated that acute H_2O_2 administration induces biphasic changes in mEPSC frequency, characterized by an initial increase followed by a prolonged depression. On the other hand, prolonged H_2O_2 administration resulted in the high frequency of mEPSC that persisted before H_2O_2 washout, suggesting that the subsequent depression of mEPSC frequency observed upon acute H_2O_2 administration is associated with the removal of H_2O_2 and does not simply reflect damage to glutamate release machinery. In addition, H_2O_2 markedly increased GABA release from presynaptic terminals at a time point coinciding with the depression in mEPSC frequency, suggesting that the latter was caused by GABA-mediated inhibitory activity. These results also indicate that H_2O_2-induced changes in excitatory and GABAergic inhibitory activities have a presynaptic origin, given that increases in mEPSC and mIPSC frequency occurred in the absence of significant changes in amplitude.

H_2O_2 increases mEPSC frequency by Ca^{2+} influx via N-type VGCCs

The results of VGCC inhibition suggested that the H_2O_2-induced increase in mEPSC frequency was due to Ca^{2+} influx mainly through N- and, to a lesser extent, P/Q- and R-type VGCCs (Fig. 8*Aa* (i)). In contrast, in hippocampal neurons, H_2O_2-induced increases in Ca^{2+} flux occur through L-type VGCCs (Akaishi *et al.* 2004) whereas in *Xenopus* oocytes, P/Q-type VGCCs are mainly involved (Li *et al.* 1998). These differences may be due

after 5 min of H_2O_2 superfusion (38.9 ± 3.2% of control, $n = 6$). *C*, summary of mEPSC frequency during (left) and after (right) H_2O_2 superfusion with TTX alone ($n = 11$) or with CSA (a MPT blocker/calcineurin inhibitor, 10 μM; $n = 6$), Dant (10 μM; $n = 5$–8), or 2-APB (200 μM; $n = 6$) relative to the control (mean ± SEM). Values on the left indicate maximal values of mEPSC frequency relative to the control 1.5–6 min after H_2O_2 superfusion. *P* values were determined by one-way ANOVA with a Bonferroni *post hoc* test. *D*, FFA (100 μM), a TRPM2 channel blocker, did not block the H_2O_2-induced increase and subsequent depression in mEPSC frequency. *E*, summary of mEPSC frequency recordings in the presence of FFA (mean ± SEM, $n = 7$). Values in the charts correspond to percentage change in maximal values of mEPSC frequency relative to the control during H_2O_2 superfusion and after washout. The *P* value was determined by a paired *t* test. The holding potential was −70 mV for all recordings. Washout indicates the 10 min period after initiating H_2O_2 washout.

to the variable expression of VGCC subtypes across cell types and/or parts of the cell. P/Q- and N-type Ca^{2+} channels are predominant in synaptic nerve terminals, but their relative expression levels vary across the nervous system given the distinct physiological and pathological roles of VGCCs (Evans & Zamponi, 2006). In hippocampal neurons, the function and regulation of subtypes depends on whether they are located on excitatory or inhibitory terminals (Potier *et al.* 1993). In inhibitory spinal neurons, P/Q-type VGCCs are primarily responsible for presynaptic Ca^{2+} influx (Takahashi & Momiyama, 1993), whereas our findings indicate that this function is attributable to N-type VGCCs at excitatory presynaptic terminals of spinal VH neurons under oxidative conditions.

H_2O_2-induced increases in mEPSC frequency are associated with intracellular Ca^{2+} release via RyR and IP_3R

Similar to the effects of several VGCC blockers, the H_2O_2-induced increase in mEPSC frequency was suppressed by antagonists of either RyR or IP_3R, both of which mediate Ca^{2+} release from the ER. These data suggest that the mechanism underlying H_2O_2-induced

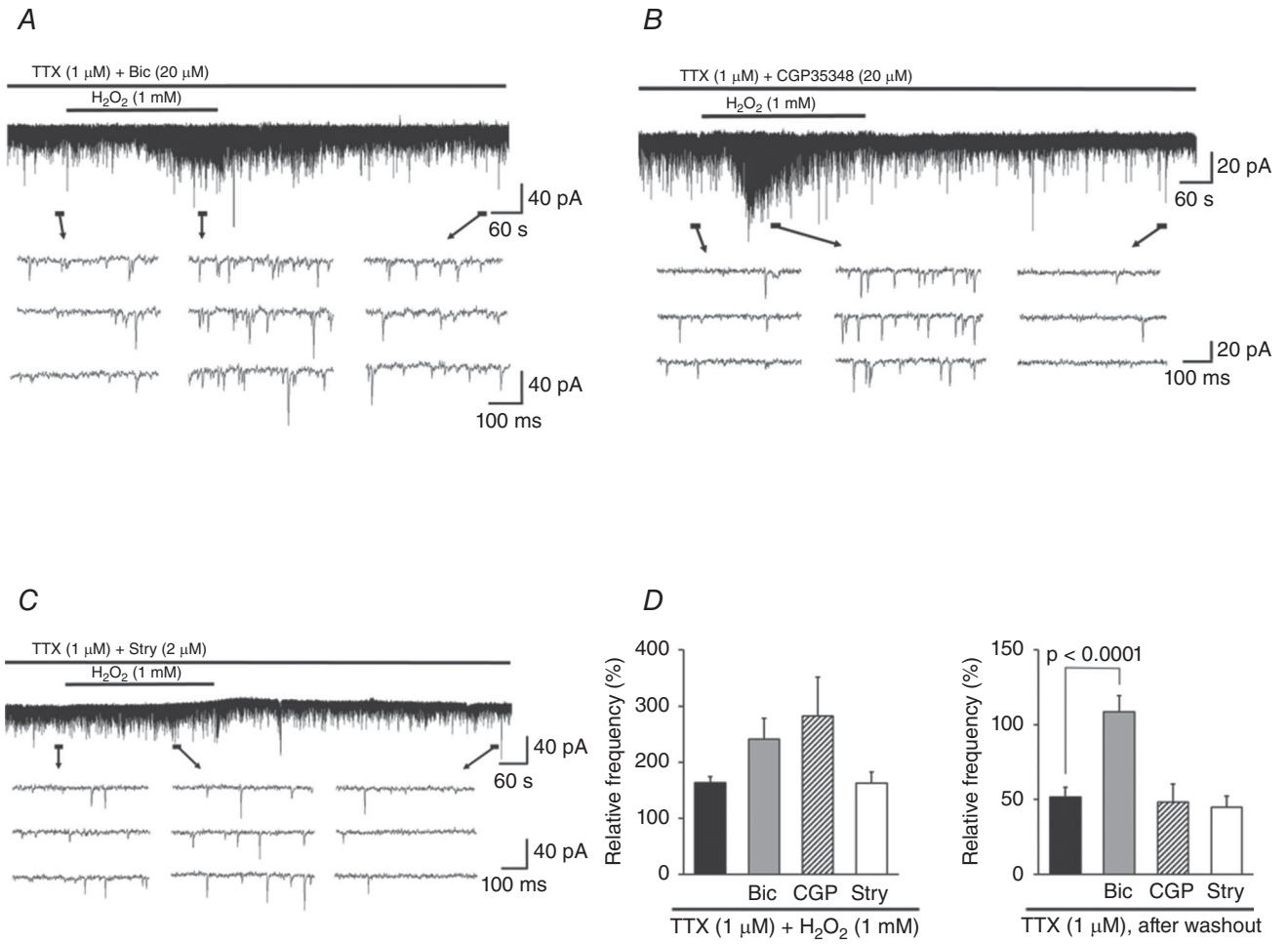

Figure 5. Effects of GABA and glycine receptor antagonists on H_2O_2-induced changes in mEPSC frequency
A, Bic (20 μM), a $GABA_A$ receptor antagonist, enhanced H_2O_2-induced increases in mEPSC frequency and blocked its subsequent depression. *B*, CGP35348 (20 μM), a $GABA_B$ receptor antagonist, enhanced the increase in frequency but had no effect on the depression. *C*, Stry (2 μM), a glycine receptor antagonist, had no effect on H_2O_2-induced changes in mEPSC frequency. *D*, summary of mEPSC frequency data during (left) and after (right) H_2O_2 superfusion with TTX alone ($n = 11$) or with Bic (20 μM; $n = 7$), CGP35348 (CGP, 20 μM; $n = 6$), or Stry (2 μM; $n = 6$) relative to the control (mean ± SEM). Values on the left indicate maximal values of mEPSC frequency relative to the control 1.5–6 min after H_2O_2 superfusion. *P* values were determined by one-way ANOVA with a Bonferroni *post hoc* test. The holding potential was −70 mV for all recordings. Washout indicates the 10 min period after initiating H_2O_2 washout.

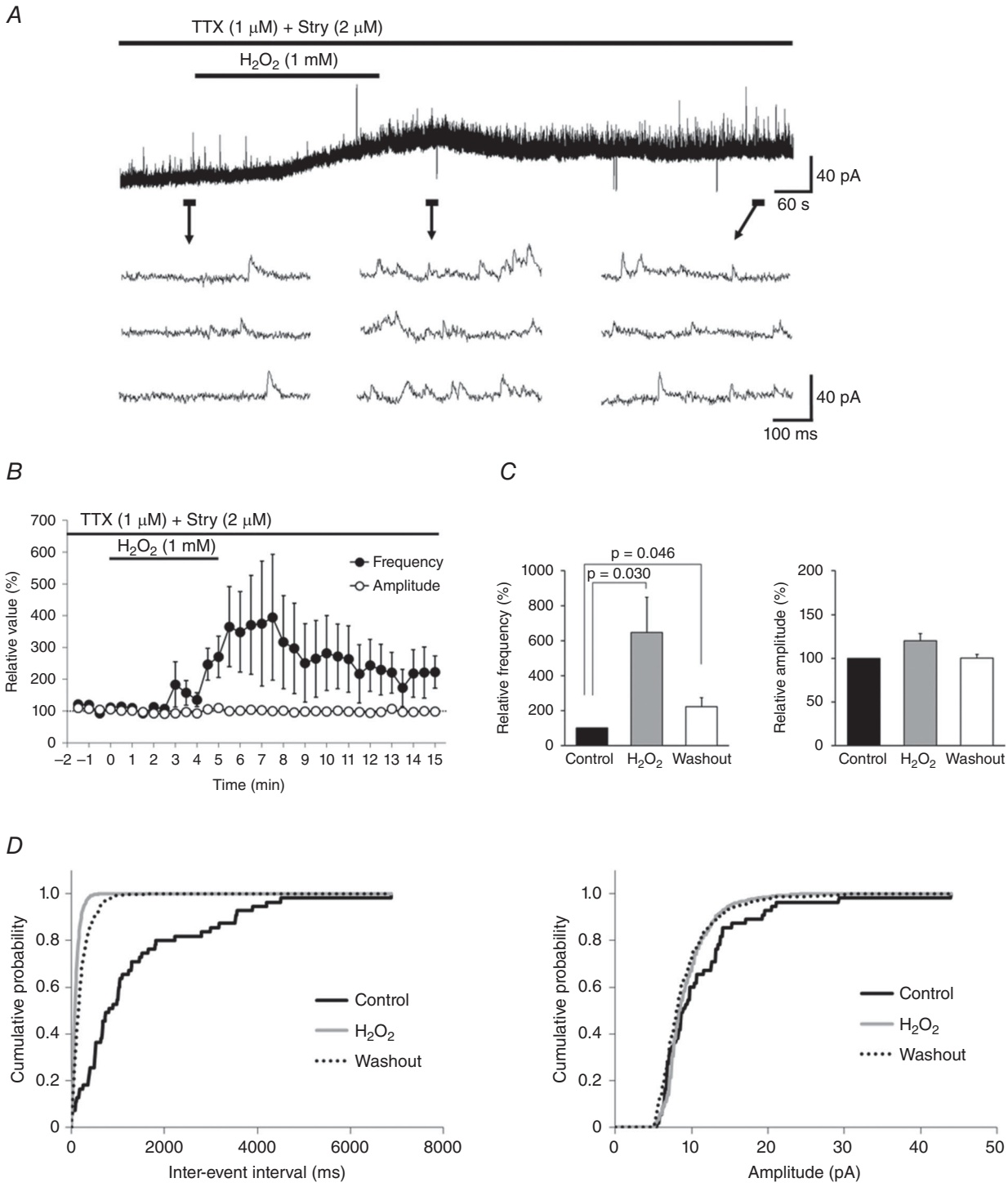

Figure 6. H_2O_2 increases the frequency of GABAergic mIPSCs
A, continuous chart recording of GABAergic mIPSCs before during, and after H_2O_2 superfusion. H_2O_2-induced increases in GABAergic mIPSC frequency were often accompanied by an outward current. *B*, average frequency (filled circles) and amplitude (open circles) of GABAergic mIPSCs after H_2O_2 superfusion relative to the control as a function of time (mean ± SEM, $n = 8$). *C*, summary of GABAergic mIPSC frequency (left) and amplitude

increases in mEPSC frequency involves Ca^{2+} release from the intracellular pool via RyR and IP_3R. Intracellular Ca^{2+}-induced Ca^{2+}-release (CICR) in response to activity is dependent on RyR and, to a lesser extent, on IP_3R. The oxidation of cysteine residues on RyR increases Ca^{2+} sensitivity, leading to excessive RyR-mediated CICR (Marengo *et al.* 1998). Our data suggest that the increase in Ca^{2+} sensitivity of RyR is responsible for the observed H_2O_2-induced increase in mEPSC frequency (Fig. 8*A* (ii)).

On the other hand, treatment with the IP_3R antagonist 2-APB blocked the H_2O_2-induced increase in mEPSC frequency, which was often accompanied by an outward current. However, blocking G-coupled protein receptor signalling, which is upstream of IP_3R, had no effect on mEPSC frequency. It was recently reported that ROS can activate IP_3 signalling and IP_3Rs by modifying cysteinyl residues, possibly in an IP_3R isoform-dependent manner (Lencesova & Krizanova, 2012; Ivanova *et al.* 2014). Thus, H_2O_2 may act directly on IP_3Rs either as a ligand or by modifying the IP_3R protein in a manner that alters Ca^{2+} release in excitatory presynaptic terminals (Fig. 8*A* (iii)). It is worth noting, however, that IP_3R antagonism did not simply inhibit H_2O_2-induced increases in mEPSC frequency but instead caused a significant reduction from the baseline value for reasons that are unclear. We speculate that activation of IP_3R-related signalling is fundamental to the increase in mEPSC frequency induced by H_2O_2, and that blocking IP_3R activated the release of neurotransmitters such as adenosine, which induced further decreases in mEPSC frequency. This is supported by previous reports that H_2O_2 activates rat hippocampal neuron adenosine A_1 receptors (Masino *et al.* 1999), leading to presynaptic inhibition of excitatory transmission and eliciting an outward current in spinal VH neurons (Miyazaki *et al.* 2008). However, it is unclear why H_2O_2 treatment in the presence of 2-APB had no effect on R_{in} even though an outward current and decrease of mEPSCs frequency were observed. The 5 mV hyperpolarizing steps we applied from a −70 mV holding potential might not be sufficient to evaluate the changes of R_{in} induced by H_2O_2 treatment in the presence of 2-APB. The precise mechanisms by which IP_3R regulates excitatory activity in spinal VH neurons, as well as the possible roles of adenosine signalling and the voltage dependency of the outward current by H_2O_2 treatment in the presence of 2-APB, remain to be elucidated.

Increases in H_2O_2-induced GABA release from presynaptic terminals is attributable to Ca^{2+} release from the IP_3R-sensitive intracellular pool

We demonstrated that presynaptic IP_3Rs have an essential role in modulating H_2O_2-induced increases in GABA release from presynaptic terminals of spinal VH neurons (Fig. 8*B* (i)). In the rat hippocampus, H_2O_2 induces Ca^{2+} release from the ER via RyR and IP_3R by acting on the redox-sensing elements of their hyper-reactive sulfhydryl groups (Gerich *et al.* 2009). In contrast, in mouse spinal dorsal horn neurons this process depends on IP_3R but not RyR (Takahashi *et al.* 2007). Thus, the two receptors have distinct roles depending on the CNS region, likely to be due to differences in expression and neuronal architecture. In addition, as observed for excitatory presynaptic terminals, blocking PLA_2/C had no effect on the H_2O_2-induced increase in GABA release, suggesting that H_2O_2 acts downstream of PLC-β (Fig. 8). However, an alternative IP_3 generating pathway may also be involved.

The H_2O_2-induced increase in GABAergic mIPSC frequency was often accompanied by an outward current. Although the underlying mechanism is unknown, this may involve hyperpolarization of the resting membrane potential by $GABA_A$ activation, which would lead to Cl^- influx into the cell body (Sivilotti & Nistri, 1991; Laube *et al.* 2002). Another possibility is that H_2O_2 increases the $GABA_A$ receptor-mediated tonic currents in hippocampal neurons (Penna *et al.* 2014). Moreover, as we used neonatal rats, an exploration of the possibility of a postsynaptic uncovering of 'silent synapses' is needed. It has been reported that silent synapses reflect the functional presence of NMDA receptors but not α-amino-3-hydroxy-5-methyl-4-isoxazole-4-propionic acid (AMPA) receptors, and that they are involved in a postsynaptic mechanism of long-term potentiation (Kerchner & Nicoll, 2008). Recently, it has been reported that there is a similar form of GABA synapse plasticity (Inoue *et al.* 2013) and that mitochondrial ROS regulates the strength of GABA-mediated synaptic transmission through a mechanism that recruits α3-containig $GABA_A$ receptors into the synapse (Accardi *et al.* 2014). Additional insight may be provided by future studies examining the postsynaptic effects of H_2O_2 including the possible involvement of silent synapses.

(right) relative to the control (mean ± SEM, $n = 8$ each) showing an increase in frequency but not amplitude induced by H_2O_2. Middle columns of charts indicate maximal values of GABAergic mIPSC frequency and amplitude relative to the control following H_2O_2 superfusion. *P* values were determined by a paired *t* test. *D*, cumulative distributions of inter-event interval (left) and amplitude (right) of GABAergic mIPSCs before (continuous black line), during (grey line), and after (dotted line) H_2O_2 superfusion. H_2O_2 did not significantly affect the distribution of amplitude (during H_2O_2 superfusion: $P = 0.051$; after washout: $P = 0.061$; Kolmogorov–Smirnov test) relative to the control, but shortened the inter-event interval during H_2O_2 superfusion and increased the interval after washout ($P < 0.0001$ for each). *A* and *D* were obtained from the same neuron. The holding potential was 0 mV for all recordings. Washout indicates the 10 min period after initiating H_2O_2 washout.

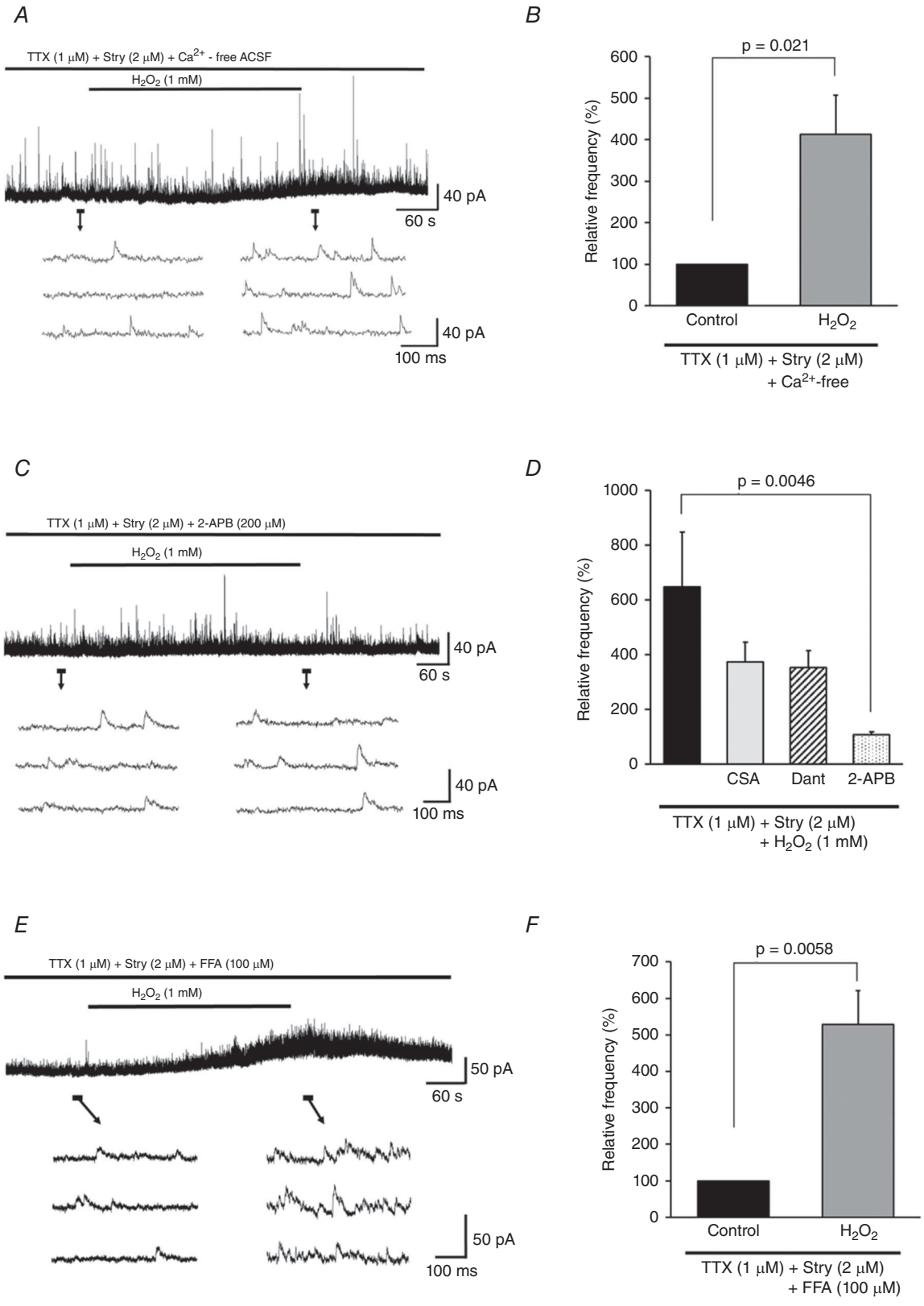

Figure 7. H_2O_2-induced increase in GABAergic mIPSC frequency is due to intracellular Ca^{2+} release via IP_3R

H_2O_2-induced increases in the frequency of mEPSC and GABAergic mIPSCs do not involve Ca^{2+} influx via TRPM2 channels

TRPM2 channels are widely expressed in the brain and have been implicated in neuronal damage induced by oxidative stress (Halliwell, 2006; Hara *et al.* 2002). Moreover, it has been reported that TRPM2 channels are also expressed in spinal VH of neonatal rats (Bianchetti *et al.* 2013) and can be activated by H_2O_2 in neuronal cells (Naziroğlu, 2011; Lee *et al.* 2011, 2013). In our acute H_2O_2 administration experiments, the TRPM2 channel blocker FFA did not block H_2O_2-induced changes in mEPSCs and GABAergic mIPSCs, suggesting that the effects of H_2O_2 do not involve Ca^{2+} influx via TRPM2 channels in spinal VH neurons.

Although the mechanism of TRPM2 channel activation by H_2O_2 is not entirely resolved, it appears that the gating mechanism relies primarily on its ability to release adenosine diphosphate ribose (ADPR) from mitochondria (Ayub & Hallett, 2004) and the nucleus (Caiafa *et al.* 2009; Esposito & Cuzzocrea, 2009; Fauzee *et al.* 2010). This suggests that exogenous H_2O_2 may be needed to cross the plasma membrane and generate ADPR from mitochondria and/or the nucleus to activate TRPM2 channels. TRPM2 activation by exogenous H_2O_2 shows slow kinetics (Sumoza-Toledo & Penner, 2011) and may therefore occur at a time point beyond our experimental range. Moreover, applying FFA for only 4 min before starting H_2O_2 superfusion might not have been sufficient to antagonize TRPM2 channels completely. Further study is needed to clarify the time dependence of FFA and H_2O_2 effects on TRPM2 channels in rat VH neurons.

H_2O_2-induced increases in GABA release inhibit glutamatergic transmission

When H_2O_2 superfusion was combined with $GABA_A$ or $GABA_B$ receptor antagonist, a robust increase in mEPSC frequency was observed. In addition, $GABA_A$ receptor antagonism blocked the depression in mEPSC frequency observed after H_2O_2 washout, indicating that this was caused by $GABA_A$ receptor activation at presynaptic terminals. These results suggest that excess GABA released from terminals may activate presynaptic $GABA_A$ and $GABA_B$ receptors of glutamatergic interneurons, thereby suppressing glutamate release and excitatory activity (Fig. 8*B* (ii)). In support of this possibility, a similar form of synaptic modulation in the cerebellar glomerulus is thought to result from GABA in single inhibitory axons (Mitchell & Silver, 2000). Nonetheless, it is unclear why subsequent depression of mEPSC frequency was blocked only by activation of $GABA_A$ receptors. One explanation is the differential distribution and physiological roles of GABA receptor subtypes in presynaptic terminals of spinal VH neurons. For example, in group Ia dorsal root afferent axons that make monosynaptic connections to motor neurons in the spinal cord, the $GABA_A$ but not the $GABA_B$ receptor, which is also present at Ia terminals, plays a predominant role in presynaptic inhibition (Stuart & Redman, 1992). Finally, as predicted by the absence of presynaptic glycine receptors in the spinal VH (Rekling *et al.* 2000), application of a glycine receptor antagonist had no effect on glutamate release induced by H_2O_2. However, as glycine is a key inhibitory transmitters in the spinal cord, the effect of H_2O_2 in glycinergic synaptic transmission should be studied.

Physiological significance of H_2O_2-induced modulation of synaptic transmission

Our results demonstrate that both glutamatergic excitatory and GABAergic inhibitory synaptic transmission were enhanced by H_2O_2-activated increases in Ca^{2+}-dependent transmitter release, albeit by different mechanisms. We do note that the apparent lack of an effect of some inhibitors might reflect the limited time (4 min) of exposure to them prior to H_2O_2 application. Notably, N-type VGCC, RyR, and IP_3R were fundamental to H_2O_2-induced increases in glutamate release, while only IP_3R was implicated in the increase in GABA release

A, H_2O_2-induced increase in GABAergic mIPSC frequency was unaffected by Ca^{2+}-free ACSF. *B*, summary of GABAergic mIPSC frequency relative to the control in Ca^{2+}-free ACSF (mean ± SEM, $n = 6$). Values in charts correspond to percentage change in maximal values of GABAergic mIPSC frequency relative to the control following H_2O_2 superfusion. *P* values were determined by a paired *t* test. *C*, H_2O_2-induced increase in GABAergic mIPSC frequency and outward current were completely blocked by 2-APB (200 μM). *D*, summary of GABAergic mIPSC frequencies observed during H_2O_2 superfusion with TTX combined with either Stry (2 μM; $n = 8$), CSA (10 μM; $n = 6$), Dant (10 μM; $n = 6$), or 2-APB (200 μM; $n = 7$) relative to the control (mean ± SEM). Maximal values of GABAergic mIPSC frequency relative to the control following H_2O_2 superfusion are shown. *P* values were determined by one-way ANOVA with a Bonferroni *post hoc* test. *E*, FFA (100 μM) did not block the H_2O_2-induced increase of GABAergic mIPSC frequency. *F*, summary of GABAergic mIPSC frequency data during FFA treatment (mean ± SEM, $n = 6$). Values in the charts correspond to the percentage change in maximal values of GABAergic mIPSC frequency relative to the control following H_2O_2 superfusion. The *P* value was determined by a paired *t* test. The holding potential was 0 mV for all recordings. Washout indicates the 10 min period after initiating H_2O_2 washout.

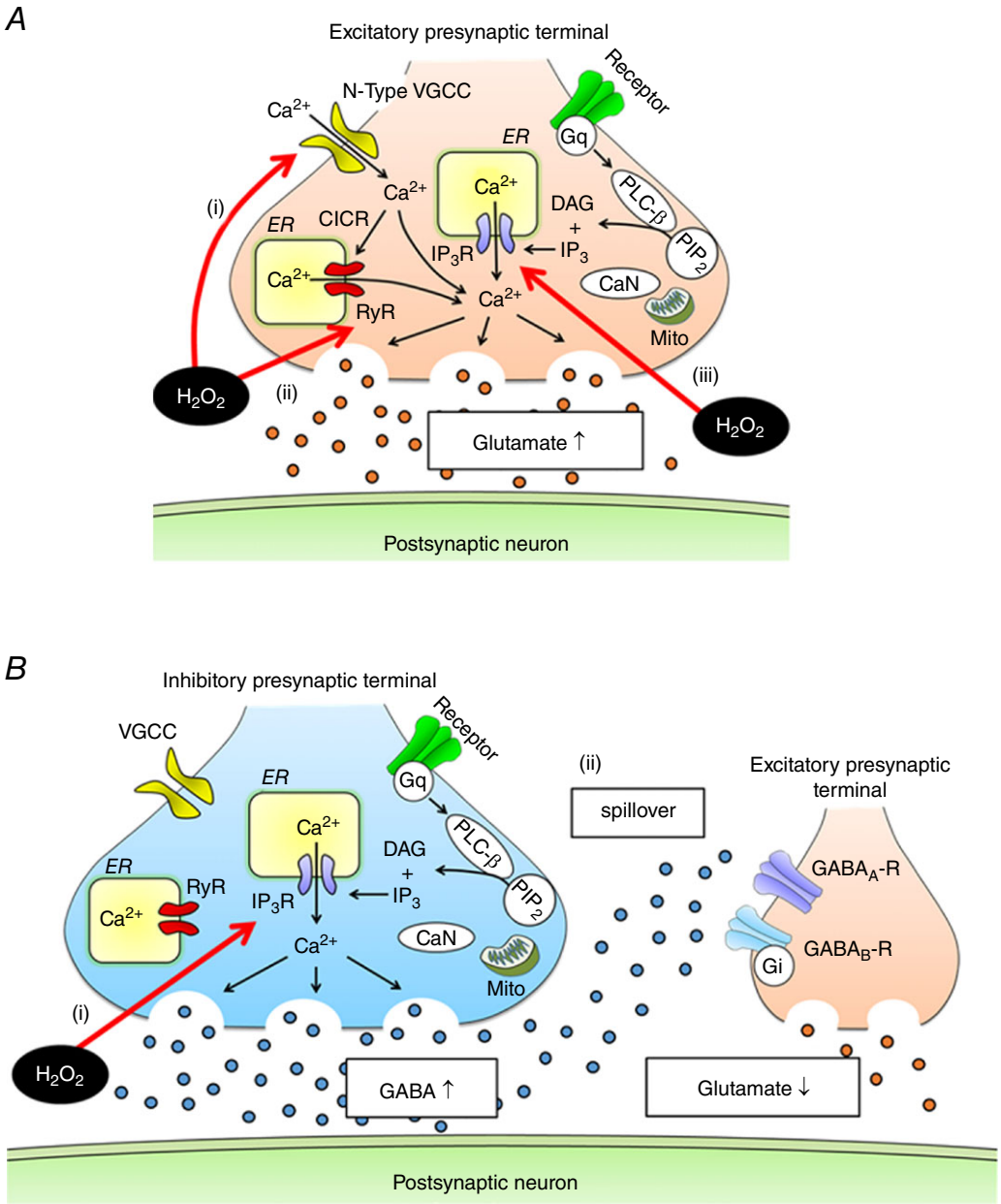

Figure 8. Model of H_2O_2-induced modulation of presynaptic activity in spinal VH neurons
A, H_2O_2 stimulates glutamate release by Ca^{2+} influx via N-type VGCC (i) and Ca^{2+} release from the ER via RyR (ii) and IP_3R (iii). Oxidation of RyR cysteine residues increases RyR sensitivity to Ca^{2+}, resulting in excessive activation of RyR-mediated CICR. The effects of H_2O_2 on IP_3R-related signalling are downstream of PLC-β. *B*, H_2O_2 increases GABAergic transmission by stimulating Ca^{2+} release from the ER via IP_3R; its site of action is downstream of PLC-β (i). Moreover, diffusion of GABA away from the release site activates presynaptic $GABA_A$ and to a lesser degree $GABA_B$ receptors (ii), thereby inhibiting glutamate release from excitatory presynaptic terminals. These effects by GABA may protect postsynaptic neurons from excitotoxicity resulting from excessive glutamate. Mito, mitochondria; CaN, calcineurin; PIP_2, phosphatidylinositol 4,5-bisphosphate; DAG, diacylglycerol.

induced by H_2O_2. These results suggest a novel strategy for preventing and/or treating H_2O_2-induced motor neuron disorders resulting from trauma or ischaemia–reperfusion injury by selectively blocking N-type VGCCs or RyR but not IP_3R, which would specifically suppress excitotoxicity caused by the H_2O_2-induced increase in glutamate release without blocking the neuroprotective effects of GABA.

References

Accardig MV, Daniels BA, Brown PM, Fritschy JM, Tyagarajan SK & Bowie D (2014). Mitochondrial reactive oxygen species regulate the strength of inhibitory GABA-mediated synaptic transmission. *Nat Commun* **5**, 3168.

Akaishi T, Nakazawa K, Sato K, Saito H, Ohno Y & Ito Y (2004). Hydrogen peroxide modulates whole cell Ca^{2+} currents through L-type channels in cultured rat dentate granule cells. *Neurosci Lett* **356**, 25–28.

Aoyama T, Koga S, Nakatsuka T, Fujita T, Goto M & Kumamoto E (2010). Excitation of rat spinal ventral horn neurons by purinergic P2X and P2Y receptor activation. *Brain Res* **1340**, 10–17.

Augustine GJ, Santamaria F & Tanaka K (2003). Local calcium signaling in neurons. *Neuron* **40**, 331–346.

Avshalumov MV & Rice ME (2002). NMDA receptor activation mediates hydrogen peroxide-induced pathophysiology in rat hippocampal slices. *J Neurophysiol* **87**, 2896–2903.

Ayub K & Hallett MB (2004). The mitochondrial ADPR link between Ca^{2+} store release and Ca^{2+} influx channel opening in immune cells. *FASEB J* **18**, 1335–1338.

Baer K, Waldvogel HJ, During MJ, Snell RG, Faull RL & Rees MI (2003). Association of gephyrin and glycine receptors in the human brainstem and spinal cord: an immunohistochemical analysis. *Neuroscience* **122**, 773–784.

Bianchetti E, Mladinic M & Nistri A (2013). Mechanisms underlying cell death in ischemia-like damage to the rat spinal cord in vitro. *Cell Death Dis* **4**, e707.

Billups B & Forsythe ID (2002). Presynaptic mitochondrial calcium sequestration influences transmission at mammalian central synapses. *J Neurosci* **22**, 5840–5847.

Caifa P, Guastafierro T & Zampieri M (2009). Epigenetics: poly(ADP-ribosyl)ation of PARP-1 regulates genomic methylation patterns. *FASEB J* **23**, 672–678.

Carri MT, Ferri A, Cozzolino M, Calabrese L & Rotilio G (2003). Neurodegeneration in amyotrophic lateral sclerosis: the role of oxidative stress and altered homeostasis of metals. *Brain Res Bull* **61**, 365–374.

Catterall WA & Few AP (2008). Calcium channel regulation and presynaptic plasticity. *Neuron* **59**, 882–901.

Coyle JT & Puttfarcken P (1993). Oxidative stress, glutamate, and neurodegenerative disorders. *Science* **262**, 689–695.

Doble A (1996). The pharmacology and mechanism of action of riluzole. *Neurology* **47**, S233–241.

Esposito E & Cuzzocrea S (2009). Superoxide, NO, peroxynitrite and PARP in circulatory shock and inflammation. *Front Biosci* **14**, 263–296.

Evans RM & Zamponi GW (2006). Presynaptic Ca^{2+} channels–integration centers for neuronal signaling pathways. *Trends Neurosci* **29**, 617–624.

Fauzee NJ, Pan J & Wang YL (2010). PARP and PARG inhibitors: new therapeutic targets in cancer treatment. *Pathol Oncol Res* **16**, 469–478.

Frank CA (2014). How voltage-gated calcium channels gate forms of homeostatic synaptic plasticity. *Front Cell Neurosci* **8**, 40.

Gerich FJ, Funke F, Hildebrandt B, Fasshauer M & Muller M (2009). H_2O_2-mediated modulation of cytosolic signaling and organelle function in rat hippocampus. *Pflugers Arch* **458**, 937–952.

Giorgio M, Trinei M, Migliaccio E & Pelicci PG (2007). Hydrogen peroxide: a metabolic by-product or a common mediator of ageing signals? *Nat Rev Mol Cell Biol* **8**, 722–728.

Halliwell B (1992). Reactive oxygen species and the central nervous system. *J Neurochem* **59**, 1609–1623.

Halliwell B (2006). Oxidative stress and neurodegeneration: where are we now? *J Neurochem* **97**, 1634–1658.

Hara Y, Wakamori M, Ishii M, Maeno E, Nishida M, Yoshida T, Yamada H, Shimizu S, Mori E, Kudoh J, Shimizu N, Kurose H, Okada Y, Imoto K & Mori Y (2002). LTRPC2 Ca^{2+}-permeable channel activated by changes in redox status confers susceptibility to cell death. *Mol Cell* **9**, 163–173.

Hill K, Benham CD, McNulty S & Randall AD (2004). Flufenamic acid is a pH-dependent antagonist of TRPM2 channels. *Neuropharmacology* **47**, 450–460.

Honda H, Baba H & Kohno T (2011). Electrophysiological analysis of vulnerability to experimental ischemia in neonatal rat spinal ventral horn neurons. *Neurosci Lett* **494**, 161–164.

Honda H, Kawasaki Y, Baba H & Kohno T (2012). The mu opioid receptor modulates neurotransmission in the rat spinal ventral horn. *Anesth Analg* **115**, 703–712.

Hyslop PA, Zhang Z, Pearson DV & Phebus LA (1995). Measurement of striatal H_2O_2 by microdialysis following global forebrain ischemia and reperfusion in the rat: correlation with the cytotoxic potential of H_2O_2 in vitro. *Brain Res* **671**, 181–186.

Inoue W, Baimoukhametova DV, Füzesi T, Wamsteeker JI, Koblinger K, Whelan PJ, Pittman QJ & Bains JS (2013). Noradrenaline is a stress-associated metaplastic signal at GABA synapses. *Nat Neurosci* **16**, 605–612.

Ivanova H, Vervliet T, Missiaen L, Parys JB, De Smedt H & Bultynck G (2014). Inositol 1,4,5-trisphosphate receptor-isoform diversity in cell death and survival. *Biochim Biophys Acta* **1843**, 2164–2183.

Jehle T, Bauer J, Blauth E, Hummel A, Darstein M, Freiman TM & Feuerstein TJ (2000). Effects of riluzole on electrically evoked neurotransmitter release. *Br J Pharmacol* **130**, 1227–1234.

Jonas P, Bischofberger J & Sandkuhler J (1998). Corelease of two fast neurotransmitters at a central synapse. *Science* **281**, 419–424.

Kawasaki Y, Fujita T & Kumamoto E (2004). Enhancement of the releases of GABA and glycine during ischemia in rat spinal dorsal horn. *Biochem Biophys Res Commun* **316**, 553–558.

Kerchner GA & Nicoll RA (2008). Silent synapses and the emergence of a postsynaptic mechanism for LTP. *Nat Rev Neurosci* **9**, 813.

Kumamoto E (1997). The pharmacology of amino-acid responses in septal neurons. *Prog Neurobiol* **52**, 197–259.

Laube B, Maksay G, Schemm R & Betz H (2002). Modulation of glycine receptor function: a novel approach for therapeutic intervention at inhibitory synapses? *Trends Pharmacol Sci* **23**, 519–527.

Leach MJ, Marden CM & Miller AA (1986). Pharmacological studies on lamotrigine, a novel potential antiepileptic drug: II. Neurochemical studies on the mechanism of action. *Epilepsia* **27**, 490–497.

Lee CR, Witkovsky P & Rice ME (2011). Regulation of substantia nigra pars reticulate GABAergic neuron activity by H_2O_2 via flufenamic acid-sensitive channels and K_{ATP} channels. *Front Syst Neurosci* **5**, 14.

Lee CR, Machold RP, Witkovsky P & Rice ME (2013). TRPM2 channels are required for NMDA-induced burst firing and contribute to H_2O_2-dependent modulation in substantia nigra pars reticulate GABAergic Neurons. *J Neurosci* **33**, 1157–1168.

Lei B, Adachi N & Arai T (1998). Measurement of the extracellular H_2O_2 in the brain by microdialysis. *Brain Res Brain Res Protoc* **3**, 33–36.

Lencesova L & Krizanova O (2012). IP_3 receptors, stress and apoptosis. *Gen Physiol Biophys* **31**, 119–130.

Li A, Segui J, Heinemann SH & Hoshi T (1998). Oxidation regulates cloned neuronal voltage-dependent Ca^{2+} channels expressed in *Xenopus* oocytes. *J Neurosci* **18**, 6740–6747.

Liu D, Liu J & Wen J (1999). Elevation of hydrogen peroxide after spinal cord injury detected by using the Fenton reaction. *Free Radic Biol Med* **27**, 478–482.

Mailly F, Marin P, Israel M, Glowinski J & Premont J (1999). Increase in external glutamate and NMDA receptor activation contribute to H_2O_2-induced neuronal apoptosis. *J Neurochem* **73**, 1181–1188.

Marengo JJ, Hidalgo C & Bull R (1998). Sulfhydryl oxidation modifies the calcium dependence of ryanodine-sensitive calcium channels of excitable cells. *Biophys J* **74**, 1263–1277.

Martin D, Thompson MA & Nadler JV (1993). The neuroprotective agent riluzole inhibits release of glutamate and aspartate from slices of hippocampal area CA1. *Eur J Pharmacol* **250**, 473–476.

Masino SA, Mesches MH, Bickford PC & Dunwiddie TV (1999). Acute peroxide treatment of rat hippocampal slices induces adenosine-mediated inhibition of excitatory transmission in area CA1. *Neurosci Lett* **274**, 91–94.

Matsumoto N, Kumamoto E, Furue H & Yoshimura M (2003). GABA-mediated inhibition of glutamate release during ischemia in substantia gelatinosa of the adult rat. *J Neurophysiol* **89**, 257–264.

Mitchell SJ & Silver RA (2000). GABA spillover from single inhibitory axons suppresses low-frequency excitatory transmission at the cerebellar glomerulus. *J Neurosci* **20**, 8651–8658.

Miyazaki N, Nakatsuka T, Takeda D, Nohda K, Inoue K & Yoshida M (2008). Adenosine modulates excitatory synaptic transmission and suppresses neuronal death induced by ischaemia in rat spinal motoneurones. *Pflugers Arch* **457**, 441–451.

Nani F, Cifra A & Nistri A (2010). Transient oxidative stress evokes early changes in the functional properties of neonatal rat hypoglossal motoneurons in vitro. *Eur J Neurosci* **31**, 951–966.

Naziroğlu M (2011). TRPM2 cation channels, oxidative stress and neurological diseases: where are we now? *Neurochem Res* **36**, 355–366.

Naziroğlu M, Özgül C, Ciğ B & Sözbir E (2011). Aminoethoxydiphenil borate and flufenamic acid inhibit Ca^{2+} influx through TRPM2 channels in rat dorsal root ganglion neurons activated by ADP-ribose and rotenone. *J Membr Biol* **241**, 69–75.

Nohda K, Nakatsuka T, Takeda D, Miyazaki N, Nishi H, Sonobe H & Yoshida M (2007). Selective vulnerability to ischemia in the rat spinal cord: a comparison between ventral and dorsal horn neurons. *Spine* **32**, 1060–1066.

Nowicky AV & Duchen MR (1998). Changes in $[Ca^{2+}]_i$ and membrane currents during impaired mitochondrial metabolism in dissociated rat hippocampal neurons. *J Physiol* **507**, 131–145.

Ornung G, Shupliakov O, Ottersen OP, Storm-Mathisen J & Cullheim S (1994). Immunohistochemical evidence for coexistence of glycine and GABA in nerve terminals on cat spinal motoneurones: an ultrastructural study. *Neuroreport* **5**, 889–892.

Pagnotta SE, Lape R, Quitadamo C & Nistri A (2005). Pre- and postsynaptic modulation of glycinergic and GABAergic transmission by muscarinic receptors on rat hypoglossal motoneurons in vitro. *Neuroscience* **130**, 783–795.

Pellegrini-Giampietro DE, Cherici G, Alesiani M, Carla V & Moroni F (1990). Excitatory amino acid release and free radical formation may cooperate in the genesis of ischemia-induced neuronal damage. *J Neurosci* **10**, 1035–1041.

Penna A, Wang DS, Yu J, Lecker I, Brown PM, Bowie D & Orser BA (2014). Hydrogen peroxide increases $GABA_A$ receptor-mediated tonic current in hippocampal neurons. *J Neurosci* **34**, 10624–10634.

Potier B, Dutar P & Lamour Y (1993). Different effects of omega-conotoxin GVIA at excitatory and inhibitory synapses in rat CA1 hippocampal neurons. *Brain Res* **616**, 236–241.

Quitadamo C, Fabbretti E, Lamanauskas N & Nistri A (2005). Activation and desensitization of neuronal nicotinic receptors modulate glutamatergic transmission on neonatal rat hypoglossal motoneurons. *Eur J Neurosci* **22**, 2723–2734.

Rekling JC, Funk GD, Bayliss DA, Dong XW & Feldman JL (2000). Synaptic control of motoneuronal excitability. *Physiol Rev* **80**, 767–852.

Rhee SG & Bae YS (1997). Regulation of phosphoinositide-specific phospholipase C isozymes. *J Biol Chem* **272**, 15045–15048.

Rice ME (2011). H_2O_2: a dynamic neuromodulator. *Neuroscientist* **17**, 389–406.

Roettger V & Lipton P (1996). Mechanism of glutamate release from rat hippocampal slices during in vitro ischemia. *Neuroscience* **75**, 677–685.

Sakurai M, Aoki M, Abe K, Sadahiro M & Tabayashi K (1997). Selective motor neuron death and heat shock protein induction after spinal cord ischemia in rabbits. *J Thorac Cardiovasc Surg* **113**, 159–164.

Schwartz-Bloom RD & Sah R (2001). γ-Aminobutyric $acid_A$ neurotransmission and cerebral ischemia. *J Neurochem* **77**, 353–371.

Shaw PJ & Ince PG (1997). Glutamate, excitotoxicity and amyotrophic lateral sclerosis. *J Neurol* **244**, S3–14.
Sivilotti L & Nistri A (1991). GABA receptor mechanisms in the central nervous system. *Prog Neurobiol* **36**, 35–92.
Stuart GJ & Redman SJ (1992). The role of $GABA_A$ and $GABA_B$ receptors in presynaptic inhibition of Ia EPSPs in cat spinal motoneurones. *J Physiol* **447**, 675–692.
Sumoza-Toledo A & Penner R (2011). TRPM2: a multifunctional ion channel for calcium signaling. *J Physiol* **589**, 1515–1525.
Taal W & Holstege JC (1994). GABA and glycine frequently colocalize in terminals on cat spinal motoneurons. *Neuroreport* **5**, 2225–2228.
Taccola G, Margaryan G, Mladinic M & Nistri A (2008). Kainate and metabolic perturbation mimicking spinal injury differentially contribute to early damage of locomotor networks in the in vitro neonatal rat spinal cord. *Neuroscience* **155**, 538–555.
Takahashi A, Mikami M & Yang J (2007). Hydrogen peroxide increases GABAergic mIPSC through presynaptic release of calcium from IP_3 receptor-sensitive stores in spinal cord substantia gelatinosa neurons. *Eur J Neurosci* **25**, 705–716.
Takahashi T (1990). Membrane currents in visually identified motoneurones of neonatal rat spinal cord. *J Physiol* **423**, 27–46.
Takahashi T & Momiyama A (1993). Different types of calcium channels mediate central synaptic transmission. *Nature* **366**, 156–158.
Thurbon D, Luscher HR, Hofstetter T & Redman SJ (1998*a*). Passive electrical properties of ventral horn neurons in rat spinal cord slices. *J Neurophysiol* **79**, 2485–2502.
Thurbon D, Luscher HR, Hofstetter T & Redman SJ (1998*b*). Passive electrical properties of ventral horn neurons in rat spinal cord slices. *J Neurophysiol* **80**, 2485–2502.
Togashi K, Inada H & Tominaga M (2008). Inhibition of the transient receptor potential cation channel TRPM2 by 2-aminoethoxydiphenyl borate (2-APB). *Br J Pharmacol* **153**, 1324–1330.
Verkhratsky A (2002). The endoplasmic reticulum and neuronal calcium signalling. *Cell Calcium* **32**, 393–404.
Westenbroek RE, Hoskins L & Catterall WA (1998). Localization of Ca^{2+} channel subtypes on rat spinal motor neurons, interneurons, and nerve terminals. *J Neurosci* **18**, 6319–6330.
Wilson JR & Fehlings MG (2014). Riluzole for acute traumatic spinal cord injury: a promising neuroprotective treatment strategy. *World Neurosurg* **81**, 825–829.
Xu SZ, Zeng F, Boulay G, Grimm C, Harteneck C & Beech DJ (2005). Block of TRPC5 channels by 2-aminoethoxydiphenyl borate: a differential, extracellular and voltage-dependent effect. *Br J Pharmacol* **145**, 405–414.
Yamamoto T, Honda H, Baba H & Kohno T (2012). Effect of xenon on excitatory and inhibitory transmission in rat spinal ventral horn neurons. *Anesthesiology* **116**, 1025–1034.
Zenisek D & Matthews G (2000). The role of mitochondria in presynaptic calcium handling at a ribbon synapse. *Neuron* **25**, 229–237.

Additional information

Competing interests

The authors have declared that no conflicts of interest exist.

Author contributions

M.O. and N.O. conducted experiments and analysed data. M.O., T.H., K.W., K.K, N.E., H.B. and T.K conceived and designed the project. M.O. and T.K. wrote the manuscript. T.H., K.W., K.K., N.O., H.B. and N.O. revised the manuscript critically for important intellectual content. All authors have approved the final version of the manuscript and agree to be accountable for all aspects of the work. All persons designated as authors qualify for authorship, and all those who qualify for authorship are listed.

Funding

This work was supported by a Grant for Promotion of Niigata University Research Projects (25C032), a Tsukada Grant for Niigata University Medical Research, and a Grant-in-Aid for Exploratory Research (grant number 25670668 and 15K19989) from the Ministry of Education, Culture, Sports, Science and Technology of Japan (Tokyo, Japan).

Acknowledgements

The authors would like to thank Yukio Sato for his technical assistance (Division of Anesthesiology, Niigata University Graduate School of Medical and Dental Sciences).